# NUMERICAL STUDY OF EFFECT OF TRIM ON PERFORMANCE OF 12500DWT CARGO SHIP USING RANSE METHOD

**Tran Quoc Chuan**[1]
**Nguyen Kim Phuong**[1]
**Tran Ngoc Tu**[1]
**Mai Van Quan**[2]
**Nguyen Duy Anh**[3,4]
**Tat-Hien Le**[3,4*]

[1] Vietnam Maritime University, Vietnam
[2] Military Institute of Ship Design, Vietnam
[3] Ho Chi Minh City University of Technology (HCMUT), Vietnam
[4] Vietnam National University Ho Chi Minh City, Vietnam

* Corresponding author: *hienlt@hcmut.edu.vn (T. Le)*

## ABSTRACT

*This paper deals with the results of studying the effect of trim on the performance of series cargo ship 12500DWT in full scale at two operating conditions by using the RANSE method. The Body Force Propeller method is used to simulate a rotating propeller behind the ship. The numerical predicted results at the ballast condition were verified and validated with sea trial data. The ship's engine power curves for different trim conditions at two operating conditions were carried out to produce a data source to evaluate the effect of trim on the performance of the 12500DWT cargo ship. The results indicate that if the ship operates under optimum trim conditions, this can decrease the ship's engine power in a range from 2.5 to 4.5% depending on different loading conditions and ship speeds. Finally, the paper also provides detailed differences in flow around the ship due to trim variation to explain the physical phenomenon of changing ship performance.*

Keywords: RANSE, Ship performance, Trim optimisation, Operating condition, Ship speed.

## INTRODUCTION

One of the issues of concern to ship owners and ship managers is reducing the operation cost of the marine transportation of cargo. For existing ships, there are some feasible measures to save energy such as improvement in voyage execution, good maintenance, weather routing, speed control, reduction of auxiliary power consumption, using an alternative control strategy for low-speed marine diesel engines, and ship trim optimisation [1-3]. Among the above measures, without changing the ship's hull shape or any additional equipment, trim optimisation is a new measure for saving fuel consumption recommended by IMO. The trim of the ship can be changed by ballasting or selecting proper loading plans.

The investigation methodology for solving the trim optimisation is based on the fact that when a ship is trimmed, the following parameters of the ship hull shape will change in comparison with the even keel condition: the submerged hull shape, especially in the bow and stern regions, and the wetted surface area. All of these issues have an impact on the flow around the ship. As a result, they affect the ship resistance and propulsive efficiency (ship performance) at a specific ship speed and loading condition. Hence, by investigating the impact of the trim on ship performance, designers could provide the master with the best trim configuration

at a certain operating condition with respect to the maximum ship performance. According to FORCE, if vessels operate in optimal trim conditions, their fuel consumption could be reduced by about 15% for certain conditions in comparison with the even keel condition. For overall fleet operations, a typical decrease in fuel consumption can range from 2.0 to 3.0% [4].

The key to solving the trim optimisation is to evaluate the ship performance accurately and efficiently. Nowadays, two common approaches that have been applied to predict the performance of the ship are model tests in a towing tank and CFD (Computational Fluid Dynamics) [5]. The latter method provides sufficient accuracy for engineering purposes. However, it is also more efficient than the former from the perspective of saving time and expense. Besides, the CFD approach is able to compute the ship performance at both model scale and full scale. Within the CFD approach, methods to evaluate the ship hydrodynamics include the panel method, the Reynolds Averaged Navier-Stokes Equations (RANSE) method, and the Large Eddy Simulation (LES) method. Recently, the most popular method has been RANSE, due to its sufficient accuracy [6-8]. Hence, this work will use the RANSE method for investigating the impact of the trim on ship performance.

A number of authors have investigated the impact of the trim on ship performance using the RANSE method. Tu et al. [9] explained the methodology for studying the effect of the trim on the resistance of the ship and applied the RANSE method for investigating this in model scale, showing good agreement between the CFD method and experimental results. Sun et al. [10] conducted trim optimisation on a 4250-TEU container ship using the RANSE method at full scale. The results showed good agreement with the experimental data. Le et al. [11] used the RANSE method to study the effect of the trim on the ship resistance at different operating conditions and concluded that the extent of the impact of the trim depends on the ship hull form and operating conditions. Evaluating the optimal trim is therefore a dynamic process. The abovementioned studies provided useful information for further research on the influence of the trim. However, those studies focus on the effect of the trim only on the ship resistance, and its influence on the propulsive efficiency in particular and on the overall ship performance is not mentioned.

In order to investigate the effect of the trim on the ship performance, it is necessary to carry out self-propulsion performance prediction at different trims. There are currently two methods for simulating the rotating propeller behind the ship, namely the discretised rotating propeller method and the body force propeller (BFP) method, used by Carrica et al. [12], Tu et al. [13], Win et al. [14] and Gokce et al. [15]. The latter method is simpler and faster at computing the self-propulsion point than the discretised rotating propeller method [15-17].

This paper deals with the effect of the trim on the performance of the ship at full scale using the RANSE method. The ship used for the study is the series 12500DWT cargo ship. The body force propeller (BFP) method is used to simulate the rotating propeller behind the ship.

## NUMERICAL SIMULATIONS

### REFERENCE VESSEL

The vessel used in this study is the cargo ship 12500DWT. The principal particulars and geometry of this ship are shown in Fig. 1 and Table 1 [18]. The reason for using this ship is that the 12500DWT cargo ship was built in large numbers in Vietnam, and their sea trial data were published in [19].

*Tab. 1. Principal particulars of the ship 12500DWT and its propeller*

| Principal particulars | | | |
|---|---|---|---|
| **Description** | | **Unit** | **Value** |
| Length of waterline | $L_{WL}$ | m | 130.51 |
| Breadth | B | m | 20.20 |
| Depth to main deck | D | m | 11.30 |
| Design draft | T | m | 8.30 |
| Volume displacement | Δ | m³ | 16050 |
| Block coefficient | $C_B$ | – | 0.742 |
| **Propeller parameters** | | | |
| Diameter of propeller | $D_P$ | m | 3.60 |
| Blade area ratio | $A_E/A_0$ | – | 0.622 |
| Hub ratio | $D_h/D_P$ | – | 0.175 |
| Number of blades | Z | – | 4 |
| Pitch ratio | $P_{0.7}/D$ | – | 0.618 |
| Direction of rotation | – | – | Right-handed |

### COMPUTATIONAL SETUP

#### Case studies

To investigate the effect of the trim on ship performance, computations were conducted for two case studies:

Case study 1: Operating condition at design draft T=8.3 m; Trim = -1.50, -1.0, -0.5, 0.0, 0.5 and 1.0 m; ship speed V=9.5, 10.5 and 11.5 knots.

Case study 2: Operating condition at ballast draft T=3.76 m; Trim = +2.20, +2.70, +3.20, +3.70, +4.20 m; ship speed V=9.50, 11.05 and 12.75 knots.

The trim of the ship is defined as the difference between the draught at the aft perpendicular ($T_A$) and forward perpendicular ($T_F$):

$$Trim = T_A - T_F \qquad (1)$$
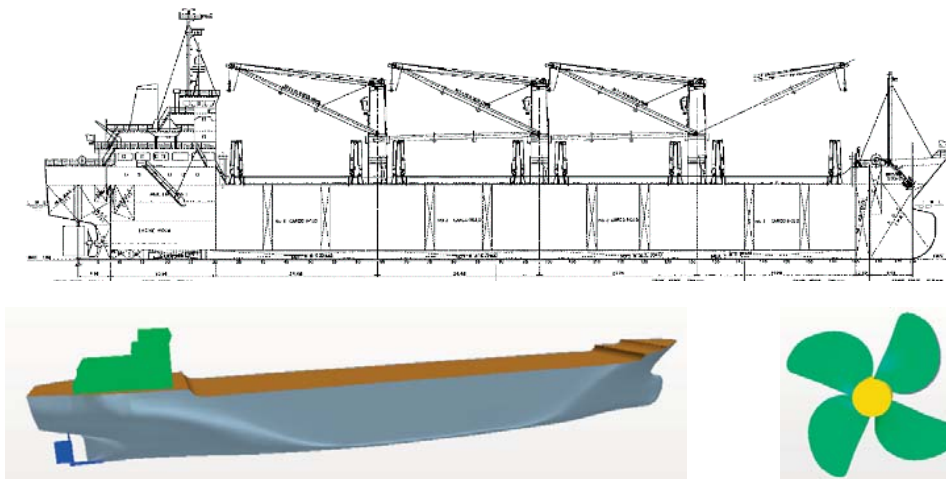
A negative value of trim means the trim by the bow.



*Fig. 1. The geometry of series 12500DWT cargo ship and its propeller*

**Numerical setup**

The setting up was conducted in conditions resembling sea trial conditions [19] as follows:
– Sea condition is calm;
– The ship is free to sink and trim;
– In the same case studies, the ship displacement is constant for different trims.

For self-propulsion simulation using the BFP method, the computational domain consists of only one region, in which there is the hull of the ship, and a virtual disc is placed in the fluid domain at the position of the ship propeller. The dimensions of the computational domain were determined based on the ITTC recommendations [20] as follows: the inlet and outlet boundaries are extended 1.5L to the bow and stern of the ship, respectively. The left and right side boundaries are extended to 2.5L from the symmetry plane of the ship. The bottom and top boundaries are placed at 2.5L and 1.25L from the free surface, respectively (see Fig. 2). The boundary conditions were set up as shown in Table 2.

The mesh used in this research was trimmed and prism layer mesh. The mesh generation process is driven by specifying the base mesh size. The mesh was refined around the hull region and near the free surface in order to capture the Kelvin wave pattern. To avoid using a fine grid in unimportant locations (far from the ship hull), local volume mesh refinement was used in the region of the virtual disc field in order to correctly capture the hull wake. The result of mesh generation is displayed in Fig. 3.

The computation was carried out using incompressible viscous RANSE. In order to close the RANSE equation, the turbulence model used in this study was SST K-ω, selected from the perspective of the level of accuracy and being less time-consuming compared with other turbulence models [21]. The 2-DOF motion was used to handle heave and pitch motions. The VOF method was employed for multi-phase flows [22].
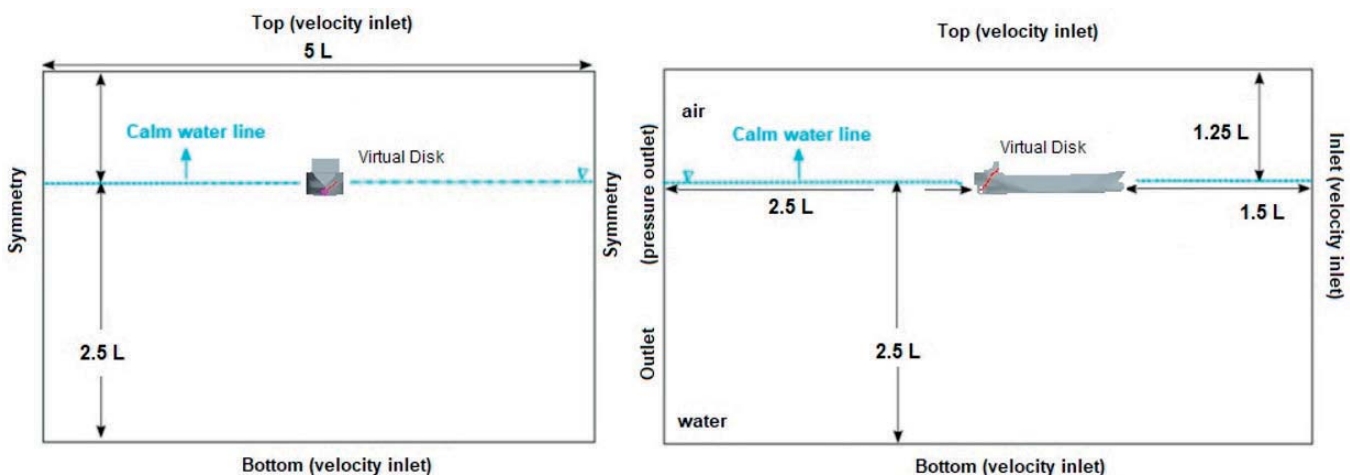


*Fig. 2. Computational domain*

Tab. 2. Boundaries and boundary conditions of self-propulsion setup using BFP method

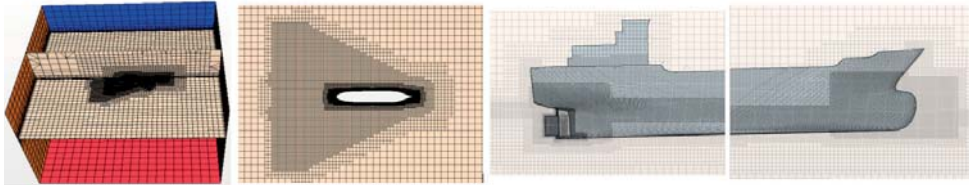| Name of boundary | Type of boundary conditions |
|---|---|
| Inlet, bottom, top | Velocity inlet |
| Outlet | Pressure outlet |
| Side left and right | Symmetry plane |
| Ship hull | No-slip wall |



Fig. 3. Result of mesh generation for self-propulsion simulation at ballast condition using BFP method

For self-propulsion simulation using the BFP method, the virtual disc is allowed to be moved with the ship. The parameters of the virtual disc of the BFP method were set based on the recommendation of [22], as shown in Table 3. The propeller's open-water performance data is taken from [17].

Tab. 3. Principal characteristics of the virtual disc parameter

| Virtual disc parameter | | Unit | Value |
|---|---|---|---|
| Inner radius | $R_h$ | m | 0.315 |
| Outer radius | $R_P$ | m | 1.800 |
| Thickness of virtual disc | t | m | $0.3R_P$ |
| Inflow plane radius | $R_I$ | m | $1.1R_P$ |
| Longitudinal position from AP | $X_{VD}$ | m | 3.25 |
| Vertical position from base line | $X_{VD}$ | m | 2.80 |

## RESULTS AND DISCUSSION

### MESH CONVERGENCE STUDY

One of the important factors that affects the numerical accuracy is the choice of grid sizes. Hence, it is necessary to carry out a mesh convergence study. A verification study for mesh sensitivity is conducted with three grids, coarse, medium, and fine, with the refinement ratio $R_i$ equal to $\sqrt{2}$ corresponding to the cell numbers of 2.82, 5.75, and 9.84 million cells respectively.

The convergence ratio is defined as follows:

$$R_G = \frac{\varepsilon_{21}}{\varepsilon_{32}}$$  (2)

where: $\varepsilon_{21} = S_2 - S_1$ is the difference between the numerical results obtained using medium ($S_2$) and fine ($S_1$) mesh; $\varepsilon_{32} = S_3 - S_2$ is the difference between the numerical results obtained using coarse ($S_3$) and medium ($S_2$) mesh.

There are three possible convergence cases: monotonic convergence ($0 < R_i < 1$), divergence ($R_i > 1$), and oscillatory convergence ($R_i < 0$).

For self-propulsion simulation using the BFP method, the mesh convergence study was performed at propeller revolution n=171 rpm and the ship speed V=11.05 knots. The numerical results obtained based on the mesh convergence study are described in Table 4, and monotonic convergence was observed. Therefore, the medium mesh was employed in further studies of self-propulsion simulations, considering also the reasonable computational effort.

Tab. 4. Results of mesh independency study for self-propulsion at V=11.05 knot and np=171 rpm

| Parameter | | Mesh density | | | ε32, % | ε12, % | RG |
|---|---|---|---|---|---|---|---|
| | | Coarse mesh (mesh #3) | Medium mesh (mesh #2) | Fine mesh (mesh #1) | | | |
| Ship resistance | $R_T$ [kN] | 161.47 | 160.80 | 160.50 | 0.42 | 0.19 | 0.45 |
| Thrust of propeller | T [kN] | 158.70 | 157.50 | 157.20 | 0.76 | 0.19 | 0.25 |
| Torque of propeller | Q [kN.m] | 113.7 | 110.80 | 110.3 | 2.62 | 0.45 | 0.17 |

## EXPERIMENTAL VALIDATION OF SHIP PERFORMANCE COMPUTATIONS

Table 5 compares the engine power from the calculation results and from sea trial data at the ballast condition. As can be seen in Table 5, the predicted engine power agrees well with the sea trial data, with a tolerance of less than 3.0%. Here the main engine power is determined as follows:

$$P_s = 2\pi n Q$$  (3)

where Q – the torque of the propeller [kN.m], n – the revolutions of the propeller [rps].

Tab. 5. Main engine power results at ballast condition in comparison to sea trial data

| Trim [m] | Ship speed [knots] | Main engine power, PS [kW] | | E%D |
|---|---|---|---|---|
| | | CFD | EFD | |
| 3.20 | 11.05 | 2036 | 1981 | 2.77% |
| 3.20 | 12.75 | 3038 | 2973 | 2.18% |

The details of flow around the ship, like wave patterns, the axial velocity field in the symmetry plane, and the axial velocity distributions in the virtual disc's plane in the self-propulsion simulation, are presented in Figs 4, 5 and 6 respectively.
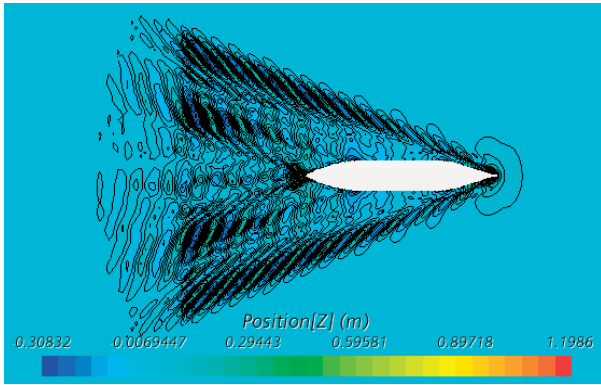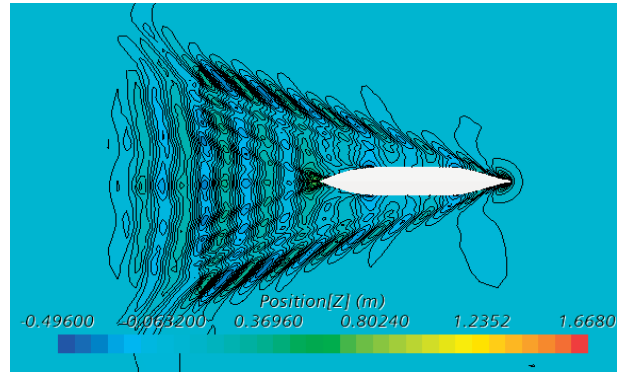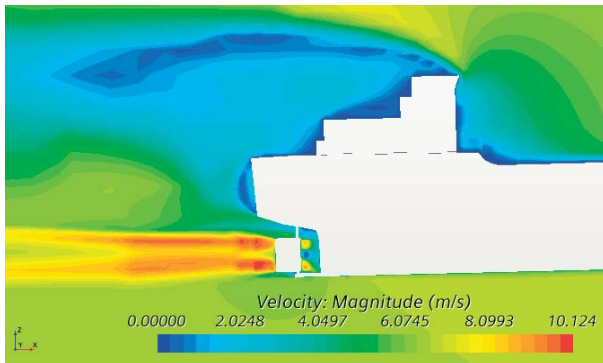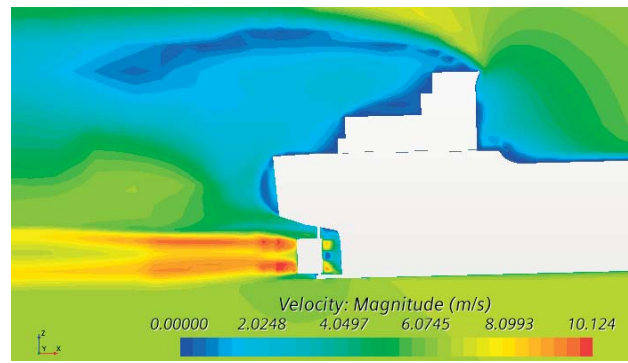
| a) V=11.05 knots | b) V=12.75 knots |

Fig. 4. Wave patterns on free surface at different ship speeds



| a) V=11.05 knots | b) V=12.75 knots |

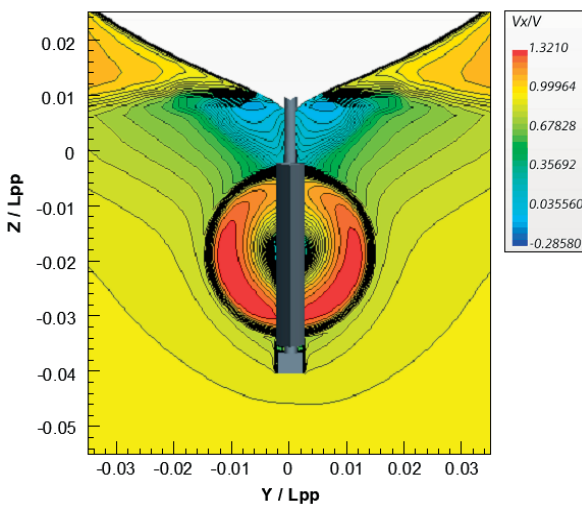Fig. 5. Axial velocity field in symmetry plane at different ship speeds



Fig. 6. Axial velocity distributions in virtual disc's plane at V=12.75 knots

## TRIM EFFECT ON SHIP PERFORMANCE AT DIFFERENT OPERATING CONDITIONS

The results of changes in the ship's engine power at different trims compared with the even keel condition (in case study 1) and with 3.20 m trim (in case study 2) are presented in Tables 6 and 7 and Figs 7 and 8. The form of the relative increase of the ship's engine power is defined as follows:

$$\Delta P_S, \% = \frac{(P_{S\_0} - P_{S\_Trim})}{P_{S\_0}} \cdot 100\% \qquad (5)$$

where: $P_{S\_0}$ – main engine power at even keel (in case study 1) and at 3.2 m trim (in case study 2); $P_{S\_Trim}$ – main engine power at different trims.

In the case of the analysed 12500DWT cargo vessel, Tables 6 and 7 and Figs 7 and 8 show that:
- Generally, there exists a relationship between the ship's trim and its engine power at each given loading condition and ship speed. When the ship runs at different trim, this will lead to a change in engine power. The trend and percentage change in the ship's main engine depend on three factors: the trim of the ship, the loading condition and ship speed.

*Tab. 6. The percentage changes of main engine power at different trims relative to even keel condition in case study 1*

| Vs [knots] | Trim, ΔT [m] | CFD computation | | | | |
|---|---|---|---|---|---|---|
| | | n [rpm] | R [kN] | Q [kN.m] | $P_s$ [kW] | ΔPs [%] |
| 9.5 | -1.50 | 159.0 | 157.8 | 88.1 | 1467 | 1.54 |
| | -1.00 | 158.5 | 156.7 | 87.4 | 1450 | 2.68 |
| | -0.50 | 159.2 | 158.2 | 88.3 | 1472 | 1.14 |
| | **0.00** | **159.7** | **159.2** | **89.0** | **1489** | **0.00** |
| | 0.50 | 160.2 | 160.2 | 89.8 | 1506 | -1.14 |
| | 1.00 | 160.5 | 160.8 | 90.1 | 1515 | -1.74 |
| 10.5 | -1.50 | 182.5 | 207.9 | 116.4 | 2225 | 2.67 |
| | -1.00 | 181.9 | 206.5 | 115.1 | 2193 | 4.06 |
| | -0.50 | 183.2 | 209.5 | 116.8 | 2242 | 1.92 |
| | **0.00** | **184.2** | **211.8** | **118.5** | **2286** | **0.00** |
| | 0.50 | 185.1 | 213.8 | 119.7 | 2320 | -1.49 |
| | 1.00 | 185.4 | 214.5 | 120.2 | 2334 | -2.11 |
| 11.5 | -1.50 | 201.1 | 252.25 | 141.1 | 2971 | 3.10 |
| | -1.00 | 200.2 | 250.05 | 139.6 | 2926 | 4.57 |
| | -0.50 | 201.6 | 253.6 | 141.7 | 2990 | 2.46 |
| | **0.00** | **203.2** | **257.6** | **144.1** | **3066** | **0.00** |
| | 0.50 | 204.2 | 260.3 | 145.9 | 3119 | -1.75 |
| | 1.00 | 204.8 | 261.8 | 146.7 | 3147 | -2.67 |

*Tab. 7. The percentage changes of main engine power at different trims relative to trim condition of 3.2 m in case study 2*

| Vs [knots] | Trim, ΔT [m] | CFD computation | | | | |
|---|---|---|---|---|---|---|
| | | n [rpm] | R [kN] | Q [kN.m] | $P_s$ [kW] | $\Delta P_s$ [%] |
| 9.50 | 2.20 | 137.66 | 104.2 | 72.42 | 1044 | -2.67 |
| | 2.70 | 136.96 | 103.2 | 71.70 | 1028 | -1.13 |
| | **3.20** | **136.45** | **102.4** | **71.16** | **1017** | **0.00** |
| | 3.70 | 135.94 | 101.6 | 70.63 | 1005 | 1.12 |
| | 4.20 | 135.53 | 101.0 | 70.20 | 996 | 2.01 |
| 11.05 | 2.20 | 174.30 | 165.9 | 115.2 | 2103 | -3.29 |
| | 2.70 | 173.40 | 163.7 | 113.9 | 2068 | -1.60 |
| | **3.20** | **172.80** | **161.5** | **112.5** | **2036** | **0.00** |
| | 3.70 | 172.00 | 159.4 | 111.3 | 2005 | 1.52 |
| | 4.20 | 171.20 | 157.0 | 110.5 | 1981 | 2.69 |
| 12.75 | 2.20 | 187.8 | 199.2 | 135.1 | 2657 | -4.34 |
| | 2.70 | 186.9 | 196.5 | 133.2 | 2607 | -2.38 |
| | **3.20** | **185.2** | **193.3** | **131.3** | **2546** | **0.00** |
| | 3.70 | 184.0 | 190.8 | 129.4 | 2493 | 2.09 |
| | 4.20 | 182.8 | 187.9 | 127.7 | 2445 | 4.00 |

In case study 1, the ship's engine power gradually decreases when the trim of the ship changes from +1.00 m to -1.00 m. In the range of trim from -1.00 m to -1.50 m, the ship's engine power increases for all 3 ship speeds. The optimum trim of the ship with respect to the minimum ship's engine power is -1.00 m. Then compared to the even keel condition, the reduction in engine power corresponding to the ship speeds of 9.5, 10.5 and 11.5 knots is 2.64, 4.03 and 4.55%, respectively (see Fig. 7).
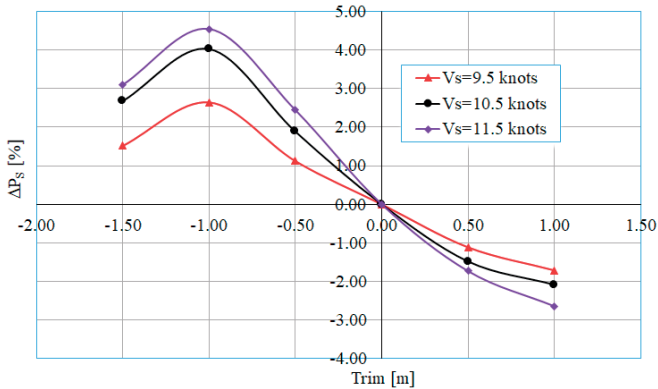


*Fig. 7. The percentage changes of main engine power at different trims relative to even keel condition in case study 1*

– When the ship runs in ballast condition (case study 2), its engine power gradually decreases when the trim of the ship changes from +2.20 m to +4.20 m. Compared with the trim value of +3.20 m (the loading state of the ship in the sea trial), increasing the trim of the ship to 4.20 m will save 2.01, 2.69 and 4.00% of power respectively corresponding to the ship's speeds of 9.5, 11.05 and 12.75 knots (see Fig. 8).
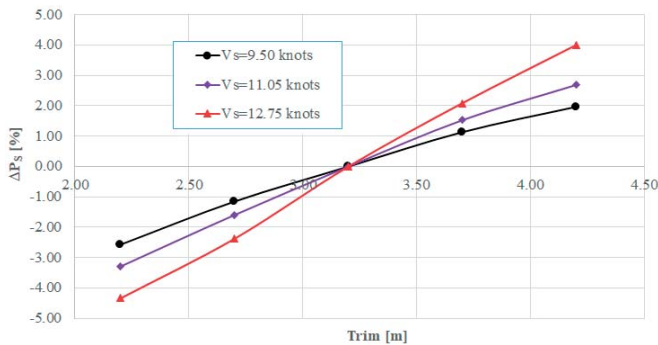


*Fig. 8. The percentage changes of main engine power at different trims relative to trim condition 3.2 m in case study 2*

The trend and level of change in the ship's engine power when varying the trim of the ship at a given loading condition and ship speed can be partly explained by the changes of the flow around the ship. For example, in case study 2, it can be seen from Figs 9 and 10 that the wave profile along the length of the ship changes monotonically with the trim of the ship. At the location of the first wave crest near the ship bow, the wave height reduces gradually when the trim of the ship changes from +2.20 m to +4.20 m. The wave has the biggest and smallest values when the trim is +2.20 m and +4.20 m,

respectively. At locations L= 95.00 m along the ship length, the height of the wave trough reduces gradually when the trim of the ship changes from +2.20 m to +4.20 m. This is one of the reasons that lead to the ship resistance in particular and the ship performance in general gradually increasing when the trim of the ship changes from +2.20 m to +4.20 m.
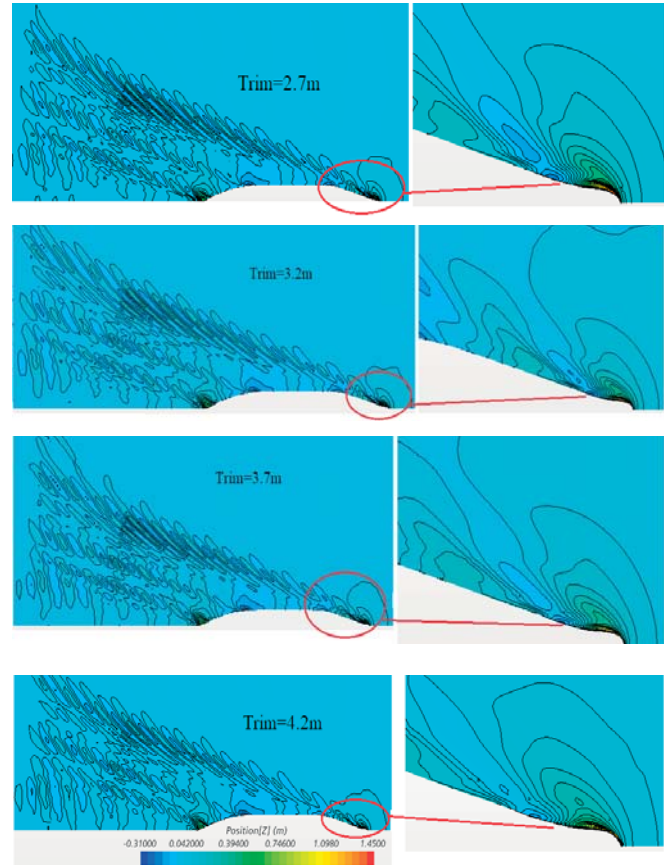


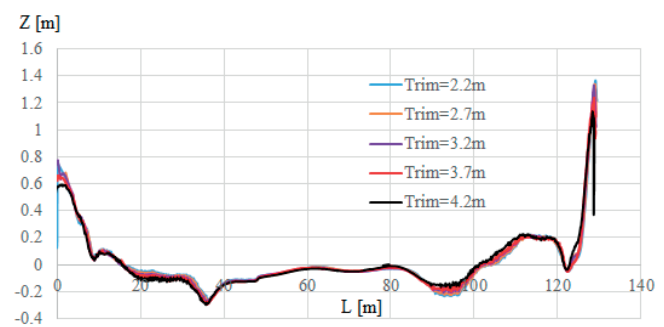*Fig. 9. Comparison of the wave patterns for various trim conditions in case study 2 at V=11.05 knots*



*Fig. 10. Comparison of the wave profile along the ship in case study 2 at V=11.05 knots*

*Fig. 11. Comparison of dynamic pressure distribution on hull surface at Z=2.7m in case study 2 with V=11.05 knots*

The resulting difference in the dynamic pressure distribution on the ship's surface with variation in the trim of the ship also provides some explanations for the changing of the ship's engine power. Fig. 11 shows the difference in the dynamic pressure distribution on the hull surface at Z=2.7 m in case study 2 with V=11.05 knots. As can be seen from this figure, there are differences in the dynamic pressure distribution on the hull surface with variation of the trim, especially at the bow and stern regions. For example, at the bow region (see Figs 12 and 13), at Z=2.70 m, the dynamic pressure increases gradually from the largest stern trim to the smallest stern trim.

# CONCLUSIONS

In this work, the unsteady RANSE method has been used with the BFP method for investigating the effect of the trim on the performance of a series cargo ship 12500DWT in full scale. To investigate this effect, two case studies with variation of the trim at different loading conditions and ship speeds are conducted. The following conclusions can be given:

– There is good agreement between the numerical results obtained and the sea trial data. This indicates the capability of the combined RANSE method and BFP method in investigating the effect of the trim on the performance of the ship.
– There is a relationship between the ship's trim and engine power at each given loading condition and ship speed. The trend and changing level in the ship's main engine depend on three factors: the trim of the ship, the loading condition and the ship speed. Hence, predicting the optimal trim of the ship is a dynamic process.
– In the case of the 12500DWT vessel analysed, there exists a certain optimal trim of the ship with respect to the maximum ship performance. Hence, studying trim optimisation is necessary in order to save energy.
– Analysing the difference in the flow field around the hull of the ship with variation of the trim of the ship provides a full understanding of the physical phenomenon of the changing ship performance at different trim conditions.
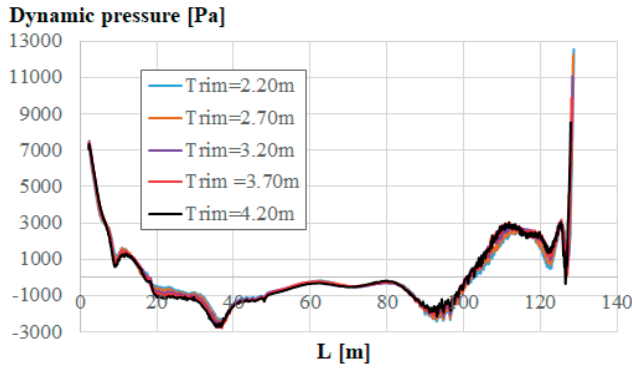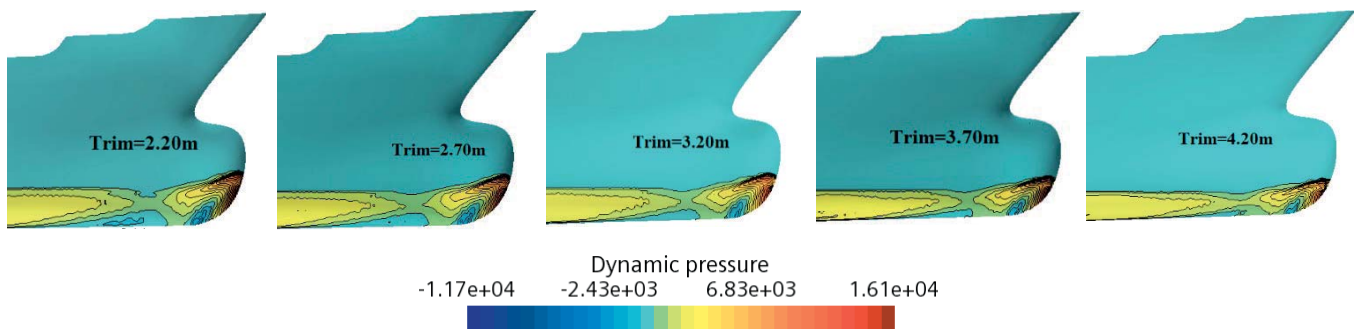


*Fig. 12. Dynamic pressure distribution on the hull form in case study 2 at V=11.05 knots*



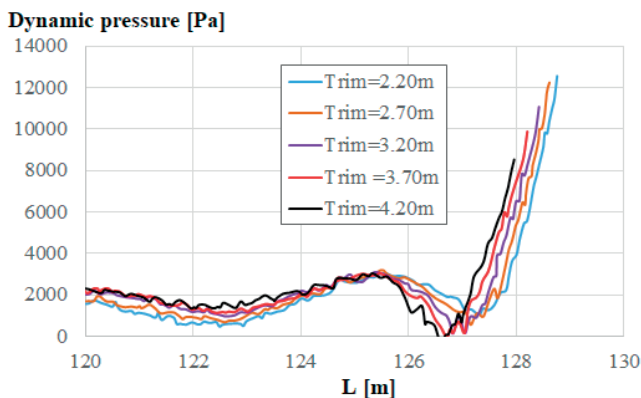*Fig. 13. Comparison of dynamic pressure distribution on fore-body in case study 2 at V=11.05 knots*

# FURTHER WORK

The present research focused on studying the effect of the trim on ship performance only in calm water conditions. Therefore, to prevent the risk of applying this measure inappropriately in ship operation, in further works, this study will be extended to investigate the influence of different sea state conditions on ship performance at different trim conditions.

# ACKNOWLEDGMENT

## REFERENCES

1. R. Vettor and C.G. Soares, *Development of a ship weather routing system.* Ocean Engineering, 2016. **123**: pp. 1-14, DOI: 10.1016/j.oceaneng.2016.06.035

2. Z. Ma, H. Chen, and Y. Zhang, *Impact of waste heat recovery systems on energy efficiency improvement of a heavy-duty diesel engine.* Archives of Thermodynamics, 2017. **38**(3): pp. 63-75, DOI: 10.1515/aoter-2017-0016.

3. H. Zeraatgar and M.H. Ghaemi, *The analysis of overall ship fuel consumption in acceleration manoeuvre using hull-propeller-engine interaction principles and governor features.* Polish Maritime Research, 2019, Vol. 26; pp. 162-173, DOI: 10.2478/pomr-2019-0018.

4. M. Reichel, A. Minchev, and N. Larsen, *Trim optimisation-theory and practice.* TransNav: International Journal on Marine Navigation and Safety of Sea Transportation, 2014. **8**, DOI 10.12716/1001.08.03.09.

5. S. Bielicki, *Prediction of ship motions in irregular waves based on response amplitude operators evaluated experimentally in noise waves.* Polish Maritime Research, 2021. Vol. 28; pp. 16-27, DOI: 10.2478/pomr-2021-0002

6. J. Choi et al., *Resistance and propulsion characteristics of various commercial ships based on CFD results.* Ocean Engineering, 2010. **37**(7): pp. 549-566, https://doi.org/10.1016/j.oceaneng.2010.02.007.

7. H. Islam and C.G. Soares, *Uncertainty analysis in ship resistance prediction using OpenFOAM.* Ocean Engineering, 2019. **191**: p. 105805. https://doi.org/10.1016/j.oceaneng.2019.02.033.

8. Y. Zhang et al., *Feasibility study of RANS in predicting propeller cavitation in behind-hull conditions.* Polish Maritime Research, 2020. DOI: 10.2478/pomr-2020-0063.

9. T.N. Tu et al., *Numerical Study on the Influence of Trim on Ship Resistance in Trim Optimization Process.* Naval Engineers Journal, 2018. **130**(4): pp. 133-142.

10. J. Sun et al., *A study on trim optimization for a container ship based on effects due to resistance.* Journal of Ship Research, 2016. **60**(1): pp. 30-47. https://doi.org/10.5957/jsr.2016.60.1.30.

11. T.-H. Le et al., *Numerical investigation on the effect of trim on ship resistance by RANSE method.* Applied Ocean Research, 2021. **111**: p. 102642. https://doi.org/10.1016/j.apor.2021.102642.

12. P.M. Carrica, A.M. Castro, and F. Stern, *Self-propulsion computations using a speed controller and a discretized propeller with dynamic overset grids.* Journal of Marine Science and Technology, 2010. **15**(4): pp. 316-330. https://doi.org/10.1007/s00773-010-0098-6.

13. T.N. Tu et al., *Numerical prediction of propeller-hull interaction characteristics using RANS method.* Polish Maritime Research, 2019, Vol. 26; pp. 163-172, DOI: 10.2478/pomr-2019-0036.

14. Y.N. Win et al., *RANS simulation of KVLCC2 using simple body-force propeller model with rudder and without rudder.* 日本船舶海洋工学会論文集, 2016. **23**: pp. 1-11. https://doi.org/10.2534/jjasnaoe.23.1

15. M.K. Gokce, O.K. Kinaci, and A.D. Alkan, *Self-propulsion estimations for a bulk carrier.* Ships and Offshore Structures, 2019. **14**(7): pp. 656-663. https://doi.org/10.1080/17445302.2018.1544108

16. Y.N. Win et al., *Computation of propeller-hull interaction using simple body-force distribution model around Series 60 CB= 0.6.* Journal of the Japan Society of Naval Architects and Ocean Engineers, 2013. **18**: pp. 17-27. https://doi.org/10.2534/jjasnaoe.18.17

17. T. Q. Chuan etal. *Full-Scale Self-propulsion Computations Using Body Force Propeller Method for Series Cargo Ship 12500DWT.* In *International Conference on Material, Machines and Methods for Sustainable Development.* 2020. Springer. https://doi.org/10.1007/978-3-030-69610-8_113

18. *Ship documents of cargo ship 12500DWT. Dongbac Shipbuilding Insdustry Joint Stock Company*

19. *Result of sea trial „Truong Minh Ocean"_12500. Dongbac Shipbuilding Insdustry Joint Stock Company.*

20. *ITTC 2014. Recommended procedures and guidelines 7.5-03-02-04.* Available from: https://ittc.info/media/4198/75-03-02-04.pdf.

21. T.N. Tu et al., *Effects of Turbulence Models on RANSE Computation of Flow Around DTMB 5415 Vessel.* Naval Engineers Journal, 2021. **133**(3): pp. 137-151.

22. *Siemens, 2020. STAR-CCM+ User Guide.*

**CONTACT WITH THE AUTHORS**

**Tran Ngoc Tu**
*e-mail: hant.dt@vimaru.edu.vn*

Vietnam Maritime University,
Lay Tray, 1800 Hai Phong,
**Vietnam**